A 2-D diode array and analysis software for verification of intensity modulated radiation therapy delivery

Paul A. Jursinic[a)]
Medical College of Wisconsin, Radiation Oncology Department, Milwaukee, Wisconsin 53792

Ben E. Nelms[b)]
TomoTherapy, Inc., Madison, Wisconsin 53717

(Received 19 November 2002; revised 22 January 2003;
accepted publication 24 February 2003; published 22 April 2003)

An analysis is made of a two-dimensional array of diodes that can be used for measuring dose generated in a plane by a radiation beam. This measuring device is the MapCHECK™ Model 1175 (Sun Nuclear, Melbourne, FL). This device has 445 N-type diodes in a 22×22 cm^2 2-D array with variable spacing. The entire array of diodes is easily calibrated to allow for measurements in absolute dose. For IMRT quality assurance, each beam is measured individually with the beam central axis oriented perpendicular to the plane of diodes. Software is available to do the analytical comparison of measurements versus dose distributions calculated by a treatment planning system. Comparison criteria of percent difference and distance-to-agreement are defined by the operator. Data are presented that show the diode array has linear response when beam fluence changes by over 300-fold, which is typical of the level of modulation in intensity modulated radiation therapy, IMRT, beams. A linear dependence is also shown for a 100-fold change in monitors units delivered. Methods for how this device can be used in the clinic for quality assurance of IMRT fields are described. Measurements of typical IMRT beams that are modulated by compensators and MLCs are presented with comparisons to treatment planning system dose calculations. A time analysis is done for typical IMRT quality assurance measurements. The setup, calibration, and analysis time for the 2-D diode array are on the order of 20 min, depending on numbers of fields. This is significantly less time than required to do similar analysis with radiographic film. The 2-D diode array is ideal for per-plan quality assurance after an IMRT system is fully commissioned. [DOI: 10.1118/1.1567831]

Key words: 2-D diode array, IMRT quality assurance, radiation therapy quality assurance

INTRODUCTION

The primary goal of radiation therapy is to deliver doses of ionizing radiation to a target, while minimizing the dose that is given to adjacent healthy tissue. How this is accomplished with external sources of radiation has evolved as significant changes in imaging, treatment planning and delivery technology have occurred in the past 20 years.[1]

Standard radiation therapy involved the use of radiation fields with approximately constant x-ray fluence across the beam.[2] Beam intensities could be modified with wedges[3] and compensator filters[4,5] as needed for 2-D and 3-D planning. Conformal radiation therapy became possible with the development of computed tomography imaging and 3-D treatment planning programs. Conformal therapy required the use of multiple, non-coplanar beams that were individually shaped to the beams-eye-view of the target.[6,7]

During the past 10 years the use of external beams with modulated fluence across the beam, intensity modulated radiation therapy, IMRT, has been introduced.[8,9] IMRT is an extension of 3-D conformal therapy that uses intensity modulated beams. This technique can produce dose distributions that have improved conformity to the target with consequent avoidance of critical structures.[10–13]

One of the challenges of radiation therapy is the establishment of quality assurance tests, which demonstrate that delivered treatments produce dose distributions as calculated by the treatment planning system. This problem is especially difficult for IMRT, which uses modulated beams that produce high dose-gradients. The ideal test would be to do true *in vivo* dosimetry and have detectors in the patient. This is not a practical solution from the patient point of view. Conventional practice, before IMRT, has relied on recommended methods for quality assurance of linear accelerators[14,15] and treatment planning systems.[15,16] Careful calibration[17] and maintenance of linear accelerators and detailed commissioning and routine checks of treatment planning systems are used in combination as an assurance of correct treatment delivery. Verification of the treatment planning systems is based on agreement of measured and computed beam profiles, depth dose curves, field-size dependence, and dose per monitor unit, MU, for a variety of field sizes for open and wedged fields.

IMRT with its highly modulated beams has required specialized dosimetric verification[18–20] in addition to what has been recommended for 2-D and 3-D conformal radiation therapy.[14–16] One method that is now commonly used[18] is to take beams that have been optimized for a patient and use them to irradiate simple-geometry phantoms. The resultant

dose distribution in the phantom is calculated by the treatment planning system and compared to the measured data. The relative dose distributions have been measured with film[18–21] and when combined with additional ion chamber measurements can be used to check absolute dosimetry. A check of the modulated beam fluence pattern[19,22] has also been carried out using a 2-D beam imaging system.

The present work characterizes a new device for measuring dose in a plane under an IMRT field. The physical and dosimetric properties are measured. Methods for how this device can be used in the clinic for quality assurance of IMRT fields and typical results are presented.

MATERIALS AND METHODS

The x-ray beam used in this work was provided by a Siemens MD2 linear accelerator. A beam with nominal energy of 6 MV was used. Absolute dose calibration of the linear accelerator was done according to TG-51[23] and this beam had a percent-depth-dose of 66.9 for x rays only at 10 cm depth in water. Calibration conditions are 1 cGy/MU set at depth-of-maximum dose of 1.6 cm, source-to-surface distance, SSD, of 98.4 cm, and a 10×10 cm^2 field defined at a distance of 100 cm. A cylindrical ion-chamber, model N30001 (PTW Hicksville, NY), calibrated at the University of Wisconsin Accredited Dosimetry Calibration Laboratory, was used in these measurements. When measuring linear accelerator outputs in air the ion chamber was covered with a cylindrical, acrylic, buildup cap with a 1.35 cm thick wall. The ion chamber was operated with 300 V of bias, which prevented measurement errors from charge-recombination.

The number of pulses produced by the linear accelerator in an irradiation was determined by the pulse counter of a Profiler, a diode linear-array detector (Sun Nuclear, Melbourne, FL). The period of the pulses was determined by dividing the irradiation time by the number of pulses counted. The pulse width was determined by measuring the time duration of the target current with an oscilloscope, Model 2247A (Tektronics, Beaverton, OR).

Scans of beam profiles were made with a three-dimensional, scanning, water-phantom system (Wellhofer Dosimetrie, Schwrazenbruck, Germany). Scans were made with a cylindrical ion chamber, Model IC-15 (Wellhofer Dosimetrie, Schwrazenbruck, Germany), which had a 0.125 cm^3 volume and a diameter of the sensitive area of 5.5 mm.

The two-dimensional dose measuring device used in this work is the MapCHECK™ Model 1175 (Sun Nuclear, Melbourne, FL). The MapCHECK consists of 445 N-type diodes that are in a 22×22 cm^2 2-D array with variable spacing between diodes, which is shown in Fig. 1. Each detector has an active area of 0.8×0.8 mm^2. These N-type diodes are a proprietary design that makes them very resistant to damage by radiation compared to N-type diodes commercially available before 2001. Two acrylic plates that have conductive surfaces envelop the diodes, which are mounted on a multilayered circuit board. This provides shielding from radio frequency fields generated in a linear accelerator and radiological buildup of 2 g/cm^2 to the detector junctions. Each detector is connected to the input of a low leakage, high gain MOSFET operational amplifier, which integrates the signal during irradiation. Signal processing is done by a personal computer connected through an amplifier interface circuit. A diode-relative-sensitivity calibration procedure, performed with a built-in software application, determines the sensitivity of each diode with respect to the central diode. The matrix of diode sensitivities is recorded as a file in the computer and is applied to subsequent diode measurements.

The entire array of diodes was calibrated in dose by the following procedure immediately before its use for IMRT beam measurements. A linear accelerator that has been calibrated according to TG-51[23] was used to irradiate the MapCHECK with a 10×10 cm^2 open field. The plane of the diodes was at 100 cm from the accelerator radiation source and the diodes were at a radiological depth of 5 g/cm^2. This was provided by 3 cm of solid water on top of the MapCHECK with its intrinsic 2 g/cm^2, 1.35 cm physical thickness, of buildup. The source-to-surface distance of this setup is 95.65 cm. The dose on the central axis at the diode plane is 92.7 cGy/100 MU for the calibrated linear accelerator. Based on the central diode reading and the matrix of diode sensitivities a built-in software application generated dose calibration factors for every detector. These factors are recorded as a file in the computer and are applied to subsequent diode measurements to give results in terms of calibrated dose.

For quality assurance of IMRT beams, the MapCHECK is used to measure every beam with the beam central axis oriented perpendicular to the plane of diodes. In order to do the measured versus calculated dose analysis, the treatment planning system must be able to use the IMRT beams (optimized for a patient) to calculate a separate dose distribution to a flat, solid-water phantom. The FOCUS 3-D Treatment Planning System (Computerized Medical Systems, St. Louis, MO) automatically calculates these quality assurance planes of dose for individual IMRT beams at a user-specified SSD and depth in phantom. In this study, the dose is calculated for a plane at 5 cm depth, which corresponds to the plane of diodes of the MapCHECK with 5 g/cm^2 buildup, and SSD of 95 cm. The dose calculation is carried out with a 3-D convolution/superposition algorithm. A software application, designed and prototyped by one of the authors, Ben Nelms, and Sun Nuclear, is available to do the analytical comparison of measured versus calculated dose. The dose distribution in the quality assurance plane is calculated at 2–3 mm resolution and interpolated to 1 mm resolution. It is viewed in the software as a grayscale ''virtual film.'' The diode array represents up to 445 point dose measurements that are superimposed on the virtual film for both percent difference and distance-to-agreement,[24] DTA, analysis. The operator can define separately a percent difference and DTA criterion (e.g., 3% percent difference/3 mm DTA, 3%/2 mm, 2%/2 mm, etc.).

Each diode reading is converted to dose, based on the calibration factors, and then compared to its corresponding

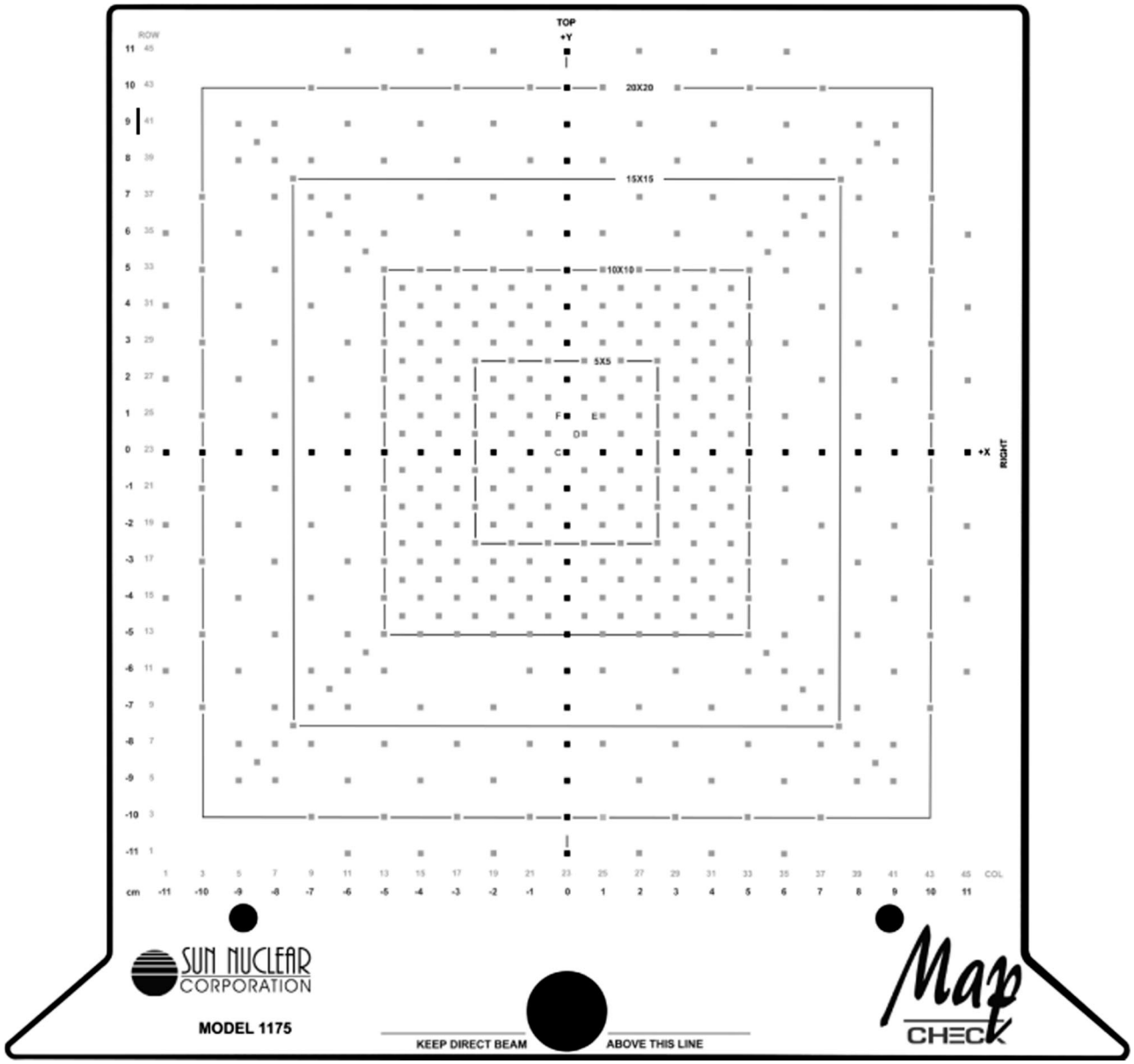

FIG. 1. The diode array pattern of the MapCHECK. The black and gray squares are the positions of the diode detectors. The center 10×10 cm^2 region has detectors spacing of 7.07 mm. The outer ring, which is 6 cm wide, has detectors spacing of 14.14 mm. The horizontal and vertical lines are 22 cm long with detector spacing of 10 mm. The diagonal lines are 25.4 cm long with detector spacing of 7.07 mm.

calculated dose value from the quality assurance dose plane. Since the measured and calculated dose are both in absolute dose, the operator need only specify the normalization (100%) dose value, and the absolute dose relationships are preserved as the dose arrays are renormalized. Each diode position is analyzed for percent difference[25] using

$$\text{Percent Difference} = \frac{100\times(\text{Dose1}-\text{Dose2})}{\text{Normalization Dose}}.$$

The DTA analysis is performed with a search of all calculated dose values in a radius around each diode position. For any given diode, if there exists within the search radius either (a) a calculated dose value equal to or (b) a calculated dose value greater than and a calculated dose value less than the measured dose, then the analysis at that point satisfies the DTA criterion.

Three different types of diode detectors were also used in this work. What is called an old N-type diode is a model 30-487-8, 6–12 MV, N-type silicon diode (Sun Nuclear, Melbourne, FL), which was manufactured prior to 2001. This diode has an intrinsic buildup cap made of brass that is suitable for 6 to 12 MV x rays. An N-type (MapCHECK) diode, which is an individual MapCHECK diode, that is packaged in a cylindrical, brass buildup cap, which is identical to that of the old N-type diode. A P-type diode, which is a model 1113000-0, is a P-type silicon diode (Sun Nuclear, Melbourne, FL). This diode has an intrinsic buildup of less

than 0.1 gm/cm^2 and is designed for dose measurements on the surface of a patient.

A model 80T-150U Universal Temperature Probe (Fluke Corp., Everett, WA) and Model 87 digital multimeter (Fluke Corp., Everett, WA) were used in combination for measuring temperature. The 80T-150U consists of a low mass, thermistor, temperature probe and a resistance-to-voltage converter.

To determine the temperature characteristics of the N-type (MapCHECK) diode it was forward biased and operated as a thermistor.[26] To do this the N-type (MapCHECK) diode was connected to the 80T-150U resistance-to-voltage converter. A voltage-temperature calibration was done as follows: the diode and a laboratory thermometer were packaged in a waterproof, latex sleeve, the combination was placed in a water bath, the temperature was varied, thermal equilibrium was established in about 7 min as evidenced by a stable voltage reading, and the temperature and voltage were measured. The voltage measured with the 80T-150U resistance-to-voltage converter was then converted to the junction-temperature of the N-type (MapCHECK) diode.

To test the diode sensitivity at various temperatures it was irradiated and the charge output was measured with a laboratory built charge integrator and amplifier. The diode was irradiated with a 10×10 cm^2, 6 MV x-ray beam. The diode was secured to the side of a water bath that had a thin-plastic wall. The temperature of the water bath was changed, thermal equilibration was allow for 5 min, and the junction temperature of the diode was monitored by measuring the forward-biased diode resistance.

RESULTS

The linear accelerator delivers dose by giving square pulses of the electron beam at a frequency of a few tenths of a kilohertz. Changing the frequency of the pulses, not the amplitude or the duration of the pulses of the electron beam, varies the dose rate of the accelerator. For 6 MV x rays on the Siemens MD2 linear, the pulse duration was measured to be 5.5 μs. A dose of 1 Gy at source-to-axis distance of 100 cm was delivered with 5723 pulses in 30 s. This is a dose per pulse, an instantaneous dose rate, of 1.75×10^{-4} Gy/pulse or 31.8 Gy/s during the pulse. The sensitivity of diodes has been shown[26–31] to change when the dose-per-pulse is of this magnitude. This has been found to be a more significant problem for N-type diodes.[26–28]

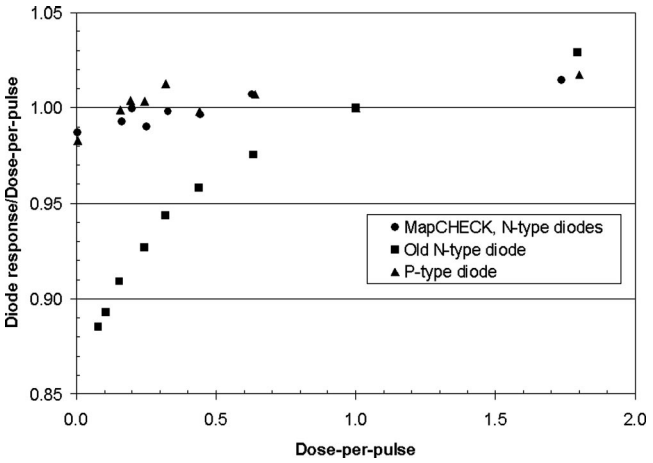

FIG. 2. Dose response of various diodes and the MapCHECK as a function of dose-per-pulse of a 6 MV x-ray beam. The MapCHECK values are an average of the five diodes in the center of the array. Exposures were made with a 10×10 cm^2 field measured at 100 cm from the radiation source of a linear accelerator. The dose-per-pulse value was varied from 1.8 to 0.16 by changing the distance of the detector to the radiation source from 75 to 250 cm. The dose-per-pulse value of 0.003 was obtained by irradiating the detector with it positioned under a collimator jaw. The total range of dose-per-pulse change is 1.8/0.003=600-fold. The dose-per-pulse values were normalized to the value at a detector-to-source distance of 100 cm. The corresponding dose-per-pulse value was 1.75×10^{-4} Gy/pulse.

The transmission of the multileaf collimator, MLC, was measured with an ion chamber at a depth of 5 cm in solid water. The ratio of the signal when the ion chamber was under the MLC to when it was in the open field was 0.3%. IMRT beams are modulated from 100% transmission to levels of 0.3%, which is the transmission of a MLC leaf. This is a potential 330-fold change in the instantaneous dose across the IMRT beam. Since the MapCHECK uses N-type diodes its dependence on dose-per-pulse is a concern.

The response of the MapCHECK and various types of

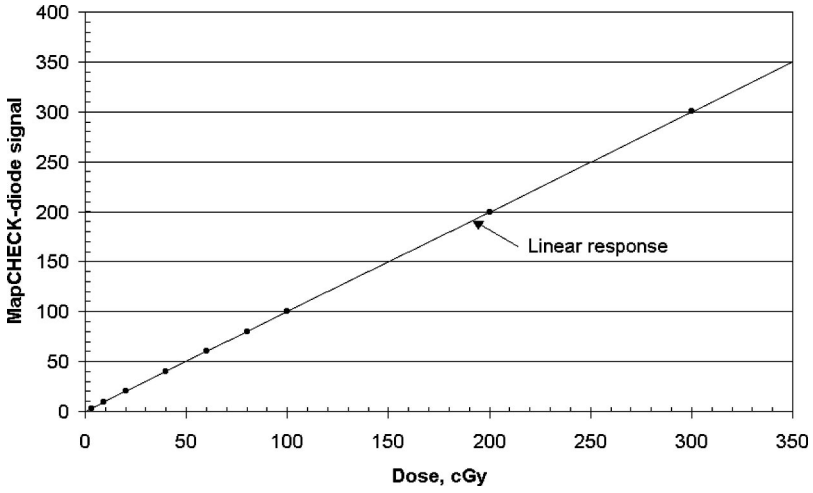

FIG. 3. Response of the MapCHECK as a function of the dose delivered. The MapCHECK values are an average of the five diodes in the center of the array. The dose was altered by changing the number of monitor units set on the accelerator.

TABLE I. Measurements of dose under an aluminum compensator shaped like a wedge. Seven repeats of this measurement were made over a 2-h period. The Cartesian coordinates, X and Y, of each diode correspond to the surface of the MapCHECK as shown in Fig. 1. These coordinates are the distance measured in the plane of the diodes.

Diode	X (cm)	Y (cm)	Average	Standard deviation	Relative standard deviation (%)
1	0	0	7838.4	2.4	0.03
2	5	0	7921.1	3.6	0.04
3	5	5	7266.9	3.0	0.04
4	0	5	7386.6	3.8	0.05
5	−5	5	7232.5	2.1	0.03
6	−5	0	7907.0	3.6	0.05
7	−5	−5	8388.5	4.5	0.05
8	0	−5	8527.1	3.0	0.04
9	5	−5	8407.6	2.6	0.03

diodes at different dose-per-pulse values are shown in Fig. 2. The value of dose-per-pulse was varied by making measurements at various distances from the source or with the detector positioned under a collimator jaw. The dose-per-pulse value itself was measured with an ion chamber. The data in Fig. 2 indicate that the MapCHECK N-type diodes are very similar to a P-type diode and have about a 2% change in sensitivity for a dose-per-pulse change of 600-fold. The old N-type diode shows greater than 14% change in its sensitivity in this same range of dose rates.

Since IMRT treatments are given at a variety of doses the response of the MapCHECK to various doses is important. The dose is what is normally referred to when making an irradiation. This is different than the dose-per-pulse described earlier. In the present context, dose is the sum of the dose delivered by each pulse in an irradiation. Figure 3 shows that the response of the MapCHECK is linear over a 100-fold change in dose.

The short-term, over a period of hours, reproducibility of MapCHECK measurements was determined by repeatedly measuring the dose under an aluminum compensator-filter, which was shaped like a wedge. The aluminum filter was irradiated by a 6 MV x-ray beam with a 15×15 cm^2 field. The MapCHECK diodes were at a source-to-axis distance of 100 cm, a radiological depth of 2 g/cm^2, and received 89 cGy on the central axis. Table I shows the result of seven repeat measurements made by nine diodes. The relative standard deviation of these measurements was $\leqslant 0.05\%$.

The long-term, over a period of months, reproducibility of MapCHECK measurements was quantified over a 261 day period of use. As explained in the Material and Methods section, a 10×10 cm^2 open field was measured prior to each measurement session. These measurements provide a record of the relative sensitivity of each diode with respect to the central diode, presuming that the beam flatness and symmetry are unchanged during this period of time. Figure 4 shows the measured relative sensitivity of four MapCHECK diodes over a 9 month period of use. Over this time period approximately 150 IMRT fields were measured with the MapCHECK with an estimated total dose delivered of 50 Gy. Based on the data in Fig. 4, there is no noticeable change in the sensitivity of these four diodes under these conditions of use. The average sensitivity and standard deviation of the data in Fig. 4 is as follows: diode 1, 1.005 ± 0.0017; diode 2, 1.004 ± 0.0018; diode 3, 1.005 ± 0.0024; and diode 4, 1.002 ± 0.0016.

The sensitivity of diodes to radiation changes with temperature. To test the MapCHECK temperature sensitivity by changing its temperature is not practical due to its large size and weight. Instead, an individual diode, N-type (MapCHECK) diode, was tested. Figure 5 shows the change in the diode signal with diode temperature. The diode temperature coefficient, C_T, at temperature, T, is defined as follows:

$$C_T(T)=\frac{1}{S(T)}\frac{dS}{dT}\bigg)_T,$$

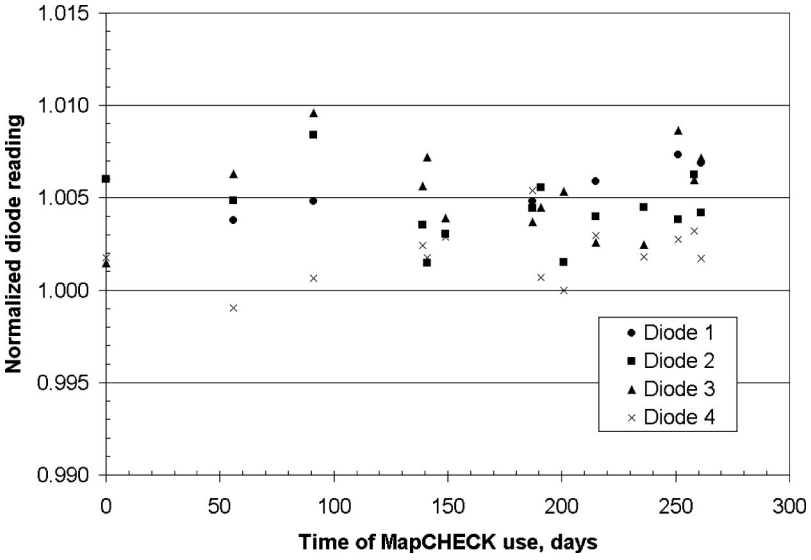

FIG. 4. The relative sensitivity of four MapCHECK diodes plotted over a period of 261 days of use. For these measurements the MapCHECK is irradiated by an open 10×10 cm^2 field as explained in the text. The measurements are for diodes with Cartesian coordinates, X and Y, that correspond to the surface of the MapCHECK as shown in Fig. 1. Measurements of diode 1 ($X=-3$,$Y=0$), diode 2 ($X=3$,$Y=0$), diode 3 ($X=0$,$Y=3$), and diode 4 ($X=0$,$Y=-3$) are shown. The diode readings are normalized by dividing them by the reading obtained by the central diode at $X=0$, $Y=0$.

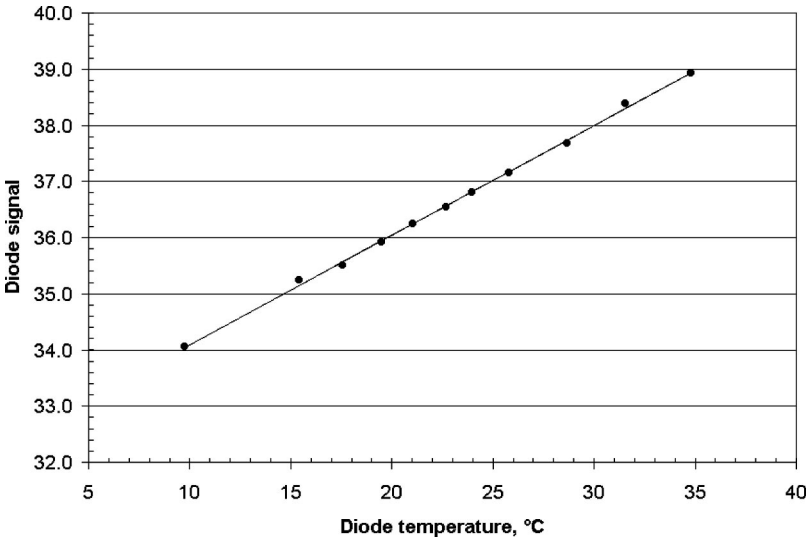

FIG. 5. The relative sensitivity of an individual N-type (MapCHECK) diode versus the temperature of the diode. The measured points are shown and the solid line is a linear fit to the data: diode signal $=32.1+0.195\times T$, where T is the temperature in °C.

where S is the diode signal. Based on the data in Fig. 5 $C_T(T=22\,^\circ\mathrm{C})=0.54\%/^\circ\mathrm{C}$.

The temperature difference across the MapCHECK was determined by measuring the surface temperature at extreme positions. These data are shown in Table II. The temperature difference is 0.1 °C across a MapCHECK that is in temperature equilibrated. Based on the measured temperature coefficient of an N-type (MapCHECK) diode this corresponds to a 0.05% difference in diode sensitivity across the MapCHECK due to temperature difference.

In order to calibrate the MapCHECK the central diode must be irradiated to a known dose. To do this requires that the scatter characteristics of the MapCHECK are known. The scatter characteristics of the MapCHECK are determined by measuring the central diode response to irradiation by different field sizes of a 6 MV x-ray beam. The same measurement is made for an ion chamber in a water phantom. These data are shown in Fig. 6. The MapCHECK central diode and the ion chamber signals increase almost identically with field size. This demonstrates that the MapCHECK and water phantom have very similar scatter characteristics. In Fig. 6 the ion chamber shows slightly greater dose rate than the MapCHECK diode at field sizes greater than $18\times18\ \mathrm{cm}^2$. This is due to a smaller amount of scatter in the MapCHECK compared to the $64\times64\times40\ \mathrm{cm}^3$ water phantom that was used. Most importantly, for a $10\times10\ \mathrm{cm}^2$ field the MapCHECK central diode and the ion chamber have virtually identical scatter behavior. Under the geometry of this measurement, the dose rate measured by the calibrated ion chamber is found to be 0.927 cGy/MU. This value is used to calibrate the MapCHECK central diode in terms of dose.

TABLE II. Measurements of the surface temperature of the MapCHECK with a low-mass thermistor. The MapCHECK was kept in a treatment room with temperature regulated to ±2 °C for 8 h before the measurements were made. In this manner, the temperature difference across the plane of the MapCHECK diodes was minimized. The Cartesian coordinates, X and Y, of each measurement point correspond to the surface of the MapCHECK as shown in Fig. 1.

X (cm)	Y (cm)	Temperature (°C)
0	0	21.6
20	0	21.6
−20	0	21.7
0	20	21.6
0	−20	21.7

The ability of the MapCHECK to measure dose across a field was compared to the profile of dose measured with an ion chamber in a water scanning-system. Figure 7 shows data for dose at a radiological depth of $2\ \mathrm{g/cm}^2$ for a $20\times20\ \mathrm{cm}^2$ field of a 6 MV x-ray beam, whose central axis is incident perpendicular to the surface of the phantom. The ''horns'' of the beam are easily seen and the MapCHECK measurements are in very close agreement to the ion chamber scan data. Figure 8 shows data for a $10\times10\ \mathrm{cm}^2$ beam, whose central axis is incident at a 30° angle to the surface of the phantom. The sloped dose distribution caused by the beam incident angle is easily seen and the MapCHECK measurements are in very close agreement to the ion chamber scan data.

Typical MapCHECK measurements and comparisons are shown in Figs. 9 and 10. These are examples of IMRT fields modulated by a MLC or a compensator. For these plots the comparison criteria of ±3% difference and a distance-to-agreement ≤3 mm were used. Since the diodes are calibrated in dose these comparisons are in absolute dose not just relative dose. Figures 11 and 12 show comparisons when the compensator was misaligned laterally or rotationally with respect to the intended dose distribution that was calculated. The MapCHECK measurement and comparison is quite sensitive to misalignments.

The use of MapCHECK for routine quality assurance of IMRT fields has been found to be very efficient. Table III gives typical values for the time needed for various steps in the measurements. The beam irradiation time is variable and depends on the type of modulation: compensator, step-and-shoot MLC, dynamic MLC, the number of intensity levels used, number of MLC segments required, and the dose that

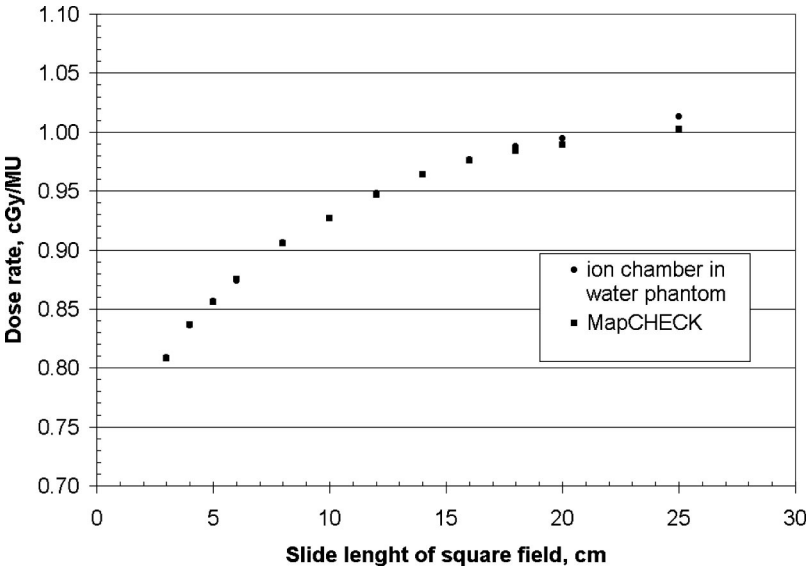

FIG. 6. The response of the MapCHECK central diode and an ion chamber versus the field size of a 6 MV x-ray beam used for irradiation. The MapCHECK diode was at source-to-axis distance of 100 cm and at a radiological depth of 5 g/cm^2. The ion chamber was at source-to-axis distance of 100 cm and at 5 cm depth in a water phantom. Dose rates were based on the response of the ion chamber, which was 0.927 cGy/MU for the 10×10 cm^2 field. The MapCHECK central diode response was normalized to this value.

is to be delivered. Since the beam irradiation time is the same for any measurement and analysis method it is neutral in any comparison. The setup, calibration, and analysis time are dependent on the analysis method. For MapCHECK these steps are on the order of 20 min, depending on numbers of fields.

DISCUSSION

Dose rate dependence has been reported to be a problem for N-type silicon diodes[26–28] but not for preirradiated P-type detectors.[28,29] It has since been shown[30,31] that P-type silicon diodes do show a dependence on dose-per-pulse, which occurs at much higher accumulated irradiation dose than for N-type diodes. The improved N-type diode used in the MapCHECK shows dose-per-pulse dependence that is quite similar to what is normally found for P-type diodes.

The radiation damage that underlies the diode dependence on dose-per-pulse increases with accumulated dose, especially from high energy photon beams that contain neutron contamination.[26,29,30,32,33] Since IMRT for head and neck sites is predominantly done with 6 MV beams, which do not have contamination neutrons, one expects a slow accumulation of radiation damage to the N-type diodes of the MapCHECK. However, if a clinic does a large number of IMRT treatments with 10–20 MV x rays, such as for prostate, then neutron damage may be important. It has been shown[33] that N- and P-type diodes have a drop in sensitivity of 1.5% to 2.2% per 1000 Gy of absorbed dose. The average IMRT treatment delivers about 2 Gy per fraction. This is approximately the dose delivered to the MapCHECK for the quality assurance check of an IMRT patient. If one allows a 2% drop in MapCHECK sensitivity before a diode-relative-sensitivity calibration is done, then the frequency of calibration would be every 500 measured patients. For most clinics, an annual calibration of the MapCHECK would be adequate.

The results displayed in Fig. 4 for 50 Gy of exposed dose

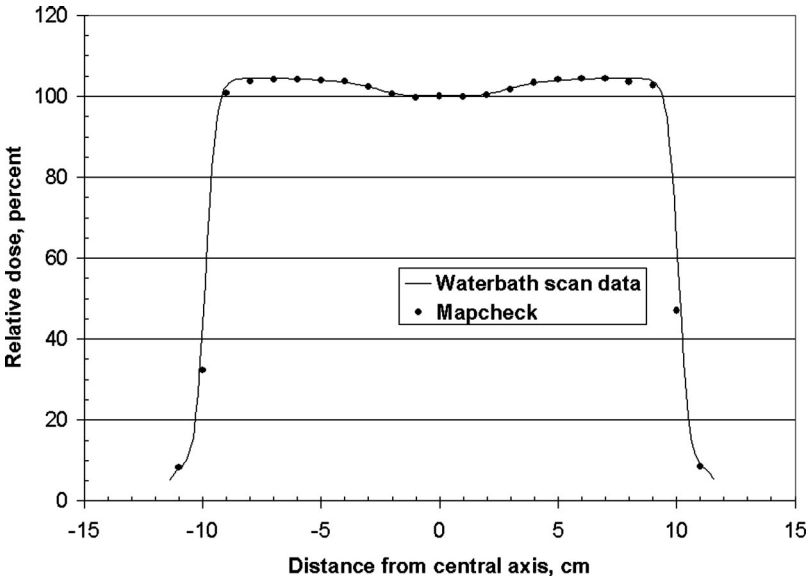

FIG. 7. A comparison of MapCHECK and ion chamber measurements of a beam profile. Irradiation is done with a 6 MV x-ray beam, 20×20 cm^2 field, whose central axis is incident perpendicular to the surface of the phantom. The ion chamber is 2 cm deep in a water phantom and measurements are shown as a solid line. The MapCHECK diodes are at a radiological depth of 2 g/cm^2. The MapCHECK diodes are along the X axis shown in Fig. 1 and measurements are shown as dots. The data are normalized to the measured value at the central axis position.

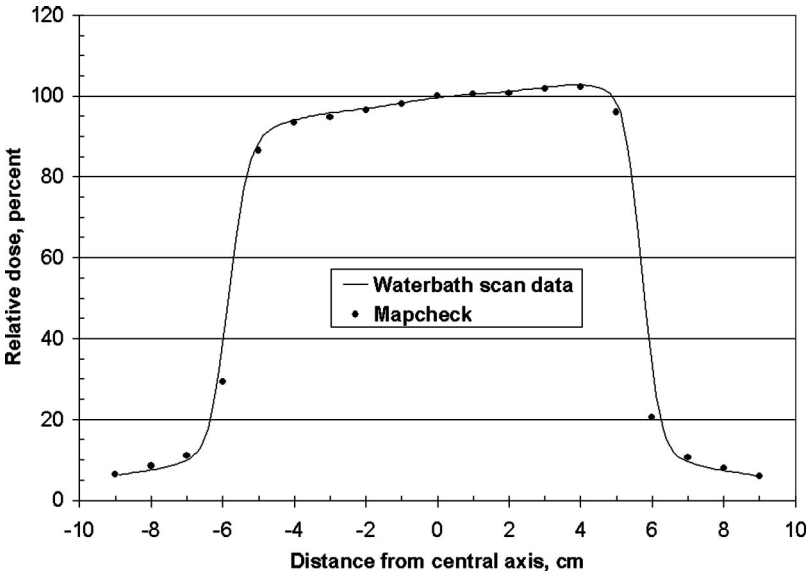

FIG. 8. A comparison of MapCHECK and ion chamber measurements of a beam profile. Irradiation is done with a 6 MV x-ray beam, 10×10 cm^2 field, whose central axis is incident at a 30° angle to the surface of the phantom. The isocenter of the beam is at depth 10 cm. The ion chamber is 10 cm deep in a water phantom and measurements are shown as a solid line. The MapCHECK diodes are at a radiological depth of 10 g/cm^2. The MapCHECK diodes are along the X axis shown in Fig. 1 and measurements are shown as dots. The data are normalized to the measured value at the central axis position.

to the MapCHECK show no discernable change in diode sensitivity. This is in agreement with earlier results[33] that would predict 0.075% to 0.11% decrease in diode sensitivity for 50 Gy of irradiation, which one could not observe above experimental uncertainty.

The temperature coefficient of the N-type (MapCHECK) diode was found to be 0.54%/°C, which is higher than the 0.05 to 0.40%/°C values reported in the literature[26,29,30,34] for N-type and P-type diodes. It is recommended that the MapCHECK be stored at a temperature close to that of the treatment room where it is going to be used. In that way temperature differences across the MapCHECK will be small as shown in Table II. Any changes in temperature in the measurement environment from day-to-day will not be important since the MapCHECK is calibrated in absolute dose immediately before a measurement session.

The comparisons done with MapCHECK measurements, such as shown in Figs. 9–12, were done with criteria of $\pm3\%$ difference and a distance-to-agreement $\leqslant3$ mm. The quantitative measurement and comparison tool that MapCHECK has allows one to ask a new question. What criteria and what percent of points passing the criteria will make a significant difference in final IMRT dose distributions and clinical outcomes? Now that this tool is available the medical physics community can attempt to answer this question.

There are two obvious advantages of using this 2-D diode array as an IMRT quality assurance tool. First is the ability to perform absolute dose comparisons for hundreds of measurement positions using only a single beam delivery, as compared to the many multitudes of delivery repetitions necessary to perform absolute point measurements with a micro ionization-chamber. Second is the efficiency in time and effort.

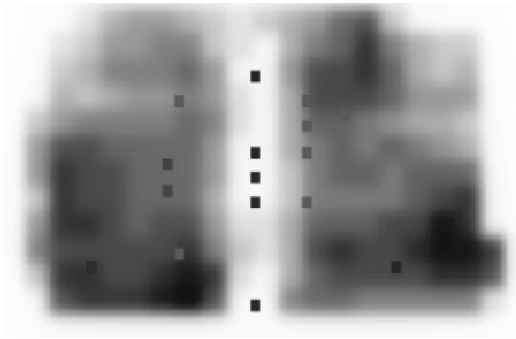

FIG. 9. A plot of the calculated dose distribution in gray scale and the comparison of the measured and calculated data for a MLC-modulated IMRT field. The points, shown as squares, in this plot indicate the location of a measured point outside the comparison criteria of $\pm3\%$ difference and a distance-to-agreement $\leqslant3$ mm. In this plot 363 points were measured with 95.6% of them meeting the comparison criteria.

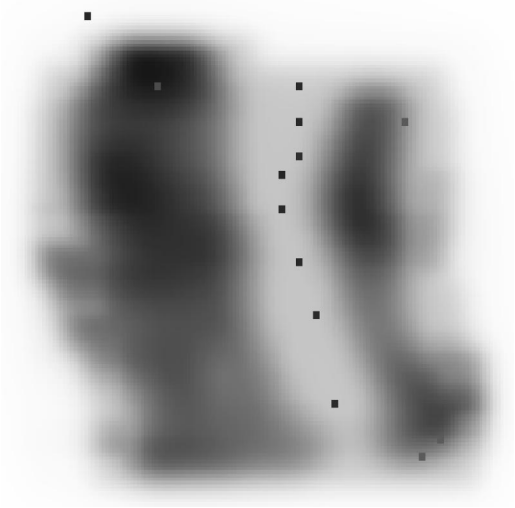

FIG. 10. A plot of the calculated dose distribution in gray scale and the comparison of the measured and calculated data for a compensator-modulated IMRT field. The points, shown as squares, in this plot indicate the location of a measured point outside the comparison criteria of $\pm3\%$ difference and a distance-to-agreement $\leqslant3$ mm. In this plot 291 points were measured with 95.5% of them meeting the comparison criteria.

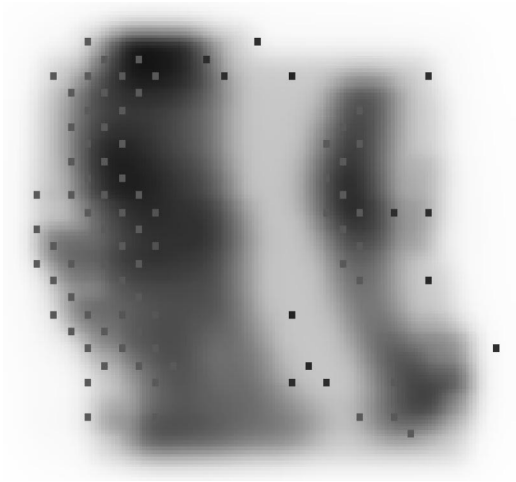

FIG. 11. A plot of the calculated dose distribution in gray scale and the comparison of the measured and calculated data for a compensator-modulated IMRT field. This plot is identical to Fig. 10 except that the compensator was misaligned by 4 mm laterally. In this plot 291 points were measured with 69.8% of them meeting the comparison criteria.

The use of MapCHECK for routine quality assurance of IMRT fields is very efficient as shown in Table III. The setup, calibration, and analysis time are on the order of 20 min, depending on numbers of fields. To do this type of quality assurance, in absolute dose, with film requires many hours of work and extreme care in processing of film, generation of the dose-response curve, and measurements of dose at a point with a calibrated ion chamber. Also, film requires an expensive 2-D film-density scanner and expensive software for converting optical density to dose and comparing the 2-D dose distribution to the dose distribution provided by the treatment-planning system.

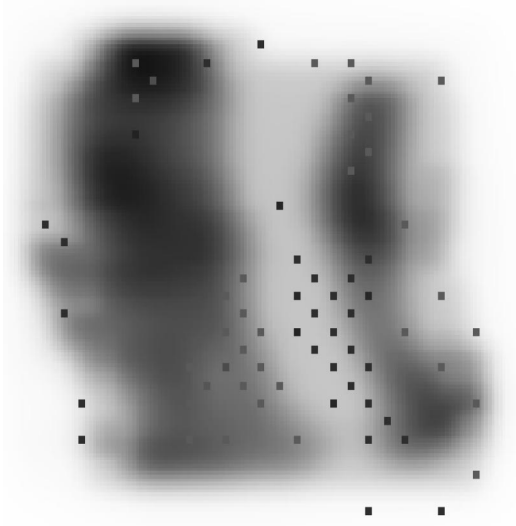

FIG. 12. A plot of the calculated dose distribution in gray scale and the comparison of the measured and calculated data for a compensator-modulated IMRT field. This plot is identical to Fig. 10 except that the compensator was misaligned by a 5° rotation around the central axis. In this plot 291 points were measured with 76.3% of them meeting the comparison criteria.

TABLE III. Analysis of time required in order to carry out quality assurance measurements with the MapCHECK.

Activity	Time (min)
Set up: connecting, computer and software startup, leveling, centering, and SSD adjustment	10
Irradiation for dose calibration	0.5
Beam irradiation per field	1 to 5
Analysis of data per field	1 to 2

One of the disadvantages of the MapCHECK is the spatial resolution of the diode array, which is shown in Fig. 1. For the 22×22 cm^2 measurement plane of the MapCHECK there are 445 measurement points. For film with assay resolution of 1 mm spacing there are 48 400 measurement points in a 22×22 cm^2 field of view. This high resolution allows film to more accurately measure regions of high dose-gradient, which occur in IMRT fields. However, as shown in Figs. 9 and 10, for routine quality assurance MapCHECK can show that measured and calculated data agree within reasonable criteria for greater than 95% of hundreds of points in the field.

The resolution of film dosimetry is unrivaled. Film is necessary in commissioning an IMRT program. However, the 2-D diode array is ideal for per-plan quality assurance after an IMRT system is fully commissioned. It would be possible to increase the resolution of the diode array by designing an accurate stepper platform to be placed under the fixed array. Multiple beam deliveries with the diode array in different positions would, in effect, provide more points of measurement that could be superimposed to give a higher resolution measurement array.

Some would argue that a major deficiency of the 2-D diode array is the inability to measure true composite plans, with the beams in their intended treatment angles incident on a measurement phantom. It is true that the diode array requires beam irradiation normal to the plane of measurement, and thus is applicable for beam-by-beam analysis rather than multi-beam composite analysis. However, beam-by-beam analysis is generally more stringent than composite analysis, as small errors in any single field are more easily detected rather than being potentially lost in a larger sea of composite dose. While composite IMRT film analysis has its merits, it is primarily popular because it reduces the time required for quality assurance by limiting the number of films irradiated, processed, calibrated, and analyzed. The 2-D diode analysis, even on a beam-by-beam basis, is much more time efficient than a single composite film analysis.

The 2-D array can also be used for routine quality assurance for open beams. The array is positioned so that diodes on the diagonals that have 7 mm separation, see Fig. 1, are parallel to the in-plane and cross-plane directions of the beam. The MapCHECK control software generates an ASCII text file of the diode measurements. A spreadsheet program[35] written for Microsoft Excel by one of the authors, PAJ, reads this file. Beam flatness, area symmetry, and light-field versus

radiation-field coincidence are determined. This is a very efficient quality assurance method since a single irradiation gives both in-plane and cross-plane data.

Also useful in the future would be a quality assurance phantom constructed to hold a 3-D array of diodes, not just a plane. Careful engineering would be required to ensure that the diodes respond equally from any direction, and there would need to be negligible perturbation of dose due to surrounding electronic circuitry. Such a volumetric phantom would provide a very efficient tool for analysis of composite IMRT plans, and would lend itself to more advanced delivery systems such as Tomotherapy or other dynamic rotational methods.

ACKNOWLEDGMENTS

The authors would like to thank the Sun Nuclear Corporation for the prototype MapCHECK used in this work and the fabrication of the individual N-type (MapCHECK) diode. Also we would like and to thank Bill Simon and Jie Shi for many useful discussions.

[a]Electronic mail: jursinic@mcw.edu
[b]Part of this work was completed while at Computerized Medical Systems, St. Louis, Missouri 63132.

[1] S. Webb, ''Three-dimensional radiation-therapy treatment planning,'' in *The Physics of Three-dimensional Radiation Therapy* (Institute of Physics Publishing, Bristol, 1993), pp. 1–64.
[2] S. H. Levitt and F. M. Khan, ''The rush to judgement: does the evidence support the enthusiasm over three-dimensional conformal radiation therapy and dose escalation in the treatment of prostate cancer?'' Int. J. Radiat. Oncol., Biol., Phys. **51**, 871–879 (2001).
[3] F. M. Khan, ''Treatment planning I,'' in *The Physics of Radiation Therapy* (Williams and Wilkins, Baltimore, 1994), pp. 226–259.
[4] F. Ellis, E. J. Hall, and R. Oliver, ''A compensator for variations in tissue thickness for high energy beams,'' Br. J. Radiol. **32**, 421–422 (1959).
[5] P. A. Jursinic, M. B. Podgorsak, and B. R. Paliwal, ''Implementation of a three-dimensional compensation system based on computed tomography generated surface contours and tissue inhomogeneities,'' Med. Phys. **21**, 357–365 (1994).
[6] D. L. McShan, B. A. Fraass, and A. S. Lichter, ''Full integration of the beam's eye view concept into computerized treatment planning,'' Int. J. Radiat. Oncol., Biol., Phys. **18**, 1485–1494 (1990).
[7] G. W. Sherouse, D. Bourland, K. Reynolds, H. L. McMurry, T. P. Mitchell, and E. L. Chaney, ''Virtual simulation in the clinical setting; Some practical considerations,'' Int. J. Radiat. Oncol., Biol., Phys. **19**, 1059–1065 (1990).
[8] S. Webb, *Intensity-Modulated Radiation Therapy* (Institute of Physics Publishing, Bristol, 2001).
[9] J. A. Purdy (Chairman of working group), ''Intensity-modulated radiation therapy: current status and issues of interest,'' Int. J. Radiat. Oncol., Biol., Phys. **51**, 880–914 (2001).
[10] R. Mohan, G. S. Mageras, B. Baldwin, L. Brewster, G. Kutcher, S. Leibel, C. M. Burnman, C. C. Ling, and Z. Fuks, ''Clinically relevant optimization of 3-D radiation treatments,'' Med. Phys. **19**, 933–944 (1992).
[11] M. P. Carol, ''Conformal radiosurgery: Stereotactic surgery and radiosurgery,'' in *3D Radiation Treatment Planning and Conformal Therapy*, edited by J. A. Purdy and B. Emami (Medical Physics, Madison, WI, 1993), pp. 249–266.
[12] C. Burman, C. Chui, G. Kutcher, S. Leibel, M. Zelefsky, T. LoSasso, S. Spirou, Q. Wu, J. Yang, J. Stein, R. Mohan, Z. Fuks, and C. C. Ling, ''Planning, delivery, and quality assurance of intensity-modulated radiotherapy using dynamic multileaf collimator: a strategy for large-scale implementation for the treatment of carcinoma of the prostate,'' Int. J. Radiat. Oncol., Biol., Phys. **39**, 863–873 (1997).
[13] M. A. Hunt, M. J. Zelefsky, S. Wolder, C. Chui, T. LoSasso, K. Rosenzweig, L. Chong, S. Spirou, L. Fromme, M. Lumley, H. A. Amols, C. C. Ling, and S. A. Leibel, ''Treatment planning and delivery of intensity-modulated radiation therapy for primary nasopharynx cancer,'' Int. J. Radiat. Oncol., Biol., Phys. **49**, 623–632 (2001).
[14] R. Nath, P. J. Biggs, F. J. Bova, C. C. Ling, J. A. Purdy, J. van de Geijn, and M. S. Weinhous, ''AAPM code of practice for radiotherapy accelerators: Report of AAPM radiation therapy task group no. 45,'' Med. Phys. **21**, 1093–1121 (1994).
[15] G. J. Kutcher, L. Coia, M. Gillin, W. F. Hanson, S. Leibel, R. J. Morton, J. R. Palta, J. A. Purdy, L. E. Reinstein, G. K. Svensson, M. Weller, and L. Wingfield, ''Comprehensive QA for radiation oncology: Report of AAPM radiation therapy committee task group 40,'' Med. Phys. **21**, 581–618 (1994).
[16] B. Fraass, K. Doppke, M. Hunt, G. Kutcher, G. Starkschell, R. Stern, and J. Van Dyke, ''American Association of Physicists in Medicine radiation therapy committee task group 53: Quality assurance for clinical radiotherapy treatment planning,'' Med. Phys. **25**, 1773–1829 (1998).
[17] P. R. Almond, P. J. Biggs, B. M. Coursey, W. F. Hanson, M. S. Huq, R. Nath, and D. W. O. Rogers, ''AAPM's TG-51 protocol for clinical reference dosimetry of high-energy photon and electron beams,'' Med. Phys. **26**, 1847–1870 (1999).
[18] J. S. Tsai, D. E. Wazer, M. N. Ling, J. K. Wu, M. Fagundes, T. DiPetrillo, B. Kramer, M. Koistinen, and M. J. Engler, ''Dosimetric verification of the dynamic intensity-modulated radiation therapy of 92 patients,'' Int. J. Radiat. Oncol., Biol., Phys. **40**, 1213–1230 (1998).
[19] L. Xing, B. Curran, R. Hill, T. Holmes, L. Ma, K. Forster, and A. L. Boyer, ''Dosimetric verification of a commercial inverse treatment planning system,'' Phys. Med. Biol. **44**, 463–478 (1999).
[20] X. R. Zhu, P. A. Jursinic, D. F. Grimm, F. Lopez, J. J. Rownd, and M. T. Gillin, ''Evaluation of Kodak EDR2 film for dose verification of intensity modulated radiation therapy delivered by a static multileaf collimator,'' Med. Phys. **29**, 1687–1692 (2002).
[21] J. Y. Ting and L. W. Davis, ''Dose verification for patient undergoing IMRT,'' Med. Dosim **26**, 205–213 (2001).
[22] L. Ma, P. B. Geis, and L. Boyer, ''Quality assurance for dynamic multileaf collimator modulated fields using a fast beam imaging system,'' Med. Phys. **24**, 1213–1220 (1997).
[23] P. R. Almond, P. J. Biggs, B. M. Coursey, W. F. Hanson, M. S. Huq, R. Nath, and D. W. O. Rogers, ''AAPM's TG-51 protocol for clinical reference dosimetry of high-energy photon and electron beams,'' Med. Phys. **26**, 1847–1870 (1999).
[24] D. A. Low, W. B. Harms, S. Mutic, and J. A. Purdy, ''A technique for the quantitative evaluation of dose distributions,'' Med. Phys. **25**, 656–661 (1998).
[25] J. Van Dyke, R. B. Barnett, J. E. Cygler, and P. C. Shragge, ''Commissioning and quality assurance of treatment planning computers,'' Int. J. Radiat. Oncol., Biol., Phys. **26**, 261–273 (1993).
[26] P. A. Jursinic, ''Implementation of an *in vivo* diode dosimetry program and changes in diode characteristics over a 4-year clinical history,'' Med. Phys. **28**, 1718–1726 (2001).
[27] E. Grusell and G. Rikner, ''Radiation damage induced dose rate nonlinearity in an N-type silicon detector,'' Acta Radiol.: Oncol. **23**, 465–469 (1984).
[28] G. Rikner and E. Grusell, ''General specifications for silicon semiconductors for use in radiation dosimetry,'' Phys. Med. Biol. **32**, 1109–1117 (1987).
[29] E. Grusell and G. Rikner, ''Linearity with dose rate of low resistivity *p*-type silicon semiconductor detectors,'' Phys. Med. Biol. **38**, 785–792 (1993).
[30] J. Van Dam, G. Leunens, and A. Dutreix, ''Correlation between temperature and dose rate dependence of semiconductor response; influence of accumulated dose,'' Radiother. Oncol. **19**, 345–351 (1990).
[31] D. Wilkins, X. A. Li, J. Cygler, and L. Gerig, ''The effect of dose rate dependence of *p*-type silicon detectors on linac relative dosimetry,'' Med. Phys. **24**, 879–881 (1997).
[32] J. Shi, ''Characteristics of the Si diode as a radiation detector for the application of in-vivo dosimetry,'' Master's thesis, Florida Institute of Technology, May 1985.
[33] A. S. Saini, T. C. Zhu, J. R. Palta, and J. Shi, ''A comparison of commercially available N- and P-type Si diode detectors,'' Med. Phys. **23**, 1071 (1996).
[34] A. S. Saini and T. C. Zhu, ''Temperature dependence of commercially available diode detectors,'' Med. Phys. **29**, 622–630 (2002).
[35] Copies of this program are available from the author.